



# PILOT INDUCED OSCILLATIONS AND FLIGHT PHASES IDENTIFICATION OF THE SPACE SHUTTLE AND TRANSPORT AIRPLANES

Sébastien Kolb<sup>1</sup>

<sup>1</sup>CREA, Centre de recherche de l'armée de l'air et de l'espace, BA 701, 13661 Salon air, France

## Abstract

In order to analyse and identify flight dynamics of the Space Shuttle and of transport airplanes, diverse mathematical tools are applied. The first item deals with rate limiting which is a major source of pilot induced oscillations. The analysis of such occurrences (so-called category II PIO) will exploit the describing function method mainly which permits to examine command channel configurations with nonlinearities. In particular, flying qualities cliffs may happen which will be diagnosed and characterized. Another topic is the identification of flight phases which covers two aspects that are the determination of unknown values for a certain model via algorithms of identification, optimization and the classification of flight phases with neural networks.

**Keywords:** pilot induced oscillations, identification, describing function method, flight dynamics

## General Introduction

Flight dynamics meets some issues which requires specific work to be treated with practical, theoretical and numerical considerations. Here two themes are our subjects of interests. The first one tries to understand the pilot induced oscillations of the Space Shuttle and the second one seeks at identifying the flight dynamics of transport airplanes. Both studies find their origin in concrete flight cases but are treated with the mathematical methodologies of nonlinear analysis and identification. At the end, valuable informations are furnished to the engineers and people who tries to have concrete figures about these issues.

### 1. Nonlinear analysis of the pilot induced oscillations of the Space Shuttle

Pilot induced oscillations due to actuator rate saturation affected diverse types of aircraft [1, 2]. Well known examples are the problems met during the developments of some fighters such as YF-16, YF-18, YF-22, Gripen or some experimental aircrafts like the X-15. But every piloted aircraft may be subject to these nefast couplings [3, 4, 5]. Nowadays strategies were developed in order to diagnose problematic configurations and to cope with such catastrophic behaviours or to alleviate them at least by modifying the flight control system. In particular, rate limiting was responsible for pilot induced oscillations of the Space Shuttle [6, 7] during the flight tests campaign in a landing phase of the flight FF-5. The nonlinear analysis of this issue will be accomplished here using the continuation of limit cycles on the one side and describing function method on the other side. The jumps corresponding to flying qualities cliffs are put in evidence mainly by observing the evolution of the limit cycle amplitudes when a control parameter changes, for example the pulsation of the forcing input oscillations or a characteristic design parameter (like overall time delay). The necessary computations are performed by making direct time simulations (figure 2), by proceeding to continuation of limit cycles but also by solving the harmonic balance equation (which involves the describing function  $N(A, \omega)$  of the nonlinearity such as equation 4). Besides it is also possible to determine the dangerous configurations depending for example on the overall time delay or to alleviate the nefast effects thanks to

modifications in the command channel like an adapted stick command shaping function in the feed-forward or a well-chosen feedback loop. From the theoretical viewpoint, diagrams of bifurcations (loci of equilibria) and locus of bifurcations points are traced to summarize the results observed in multiple time simulations. From the practical viewpoint, advices for pilots and engineers are explicated.

### 1.1 Equivalent rate limiting and describing function method

For a nonlinear element, the classical linear representation with a (linear time-invariant) transfer function which depends only on pulsation is replaced by an amplitude dependent gain, the so-called describing function  $N(A, \omega)$ . An underlying assumption for this quasi-linearization is that studying the first low-frequency harmonic is sufficient to determine the characteristics of the system such as the existence of periodical orbit, its amplitude, pulsation, etc. Indeed, it is supposed that the first harmonic concentrates all the energy, information and that the other subharmonics are negligible (filter hypothesis stating that the linear element satisfies the low-pass filter condition and that the higher harmonics are filtered out). DFM works reasonably well for this type of applications but there remain some restrictions or caveats when employing this method of which we need to be aware.

In order to examine a command channel with a a rate limiter, this last one can be taken as is but can also be replaced by an equivalent scheme [2, 1] with a saturation and an integrator (and an actuator bandwidth  $\omega_a$ ) like in figure 1.

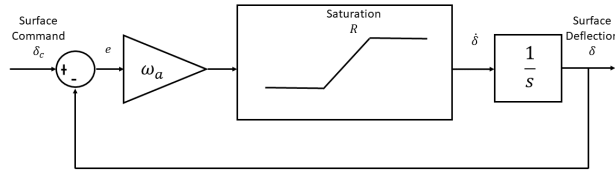


Figure 1 – Equivalent rate limiter.

As far as the DFM of a rate limiter is concerned, there exist several mathematical results which can be exploited in order to analyze the system more easily [8, 1, 2].

The effect of saturation begins to be effective for a rate limit  $R$  at an onset frequency/pulsation  $\omega_{onset}$  verifying [8]

$$R = A_{rle} \omega_{onset} = u_{stick\ input} F_{stick\ input}^{rle} (j\omega_{onset}) \omega_{onset} \quad (1)$$

where  $F_{stick\ input}^{rle} (j\omega)$  is the transfer function corresponding to rate limiter entry (rle) over stick input.

When fully saturated, the describing function of the rate limiter is [1]:

$$N(A, \omega) = \frac{4}{\pi} \frac{R}{A\omega} \exp \left( -j \arccos \left( \frac{\pi R}{2 A\omega} \right) \right) \quad (2)$$

It is also possible instead of rate limiting to employ the equivalent scheme with a position saturation whose describing function is real [9] (with the saturation value  $R$ ):

$$N(A) = \frac{2}{\pi} \left( \arcsin \frac{R}{A} + \frac{R}{A} \sqrt{1 - \left( \frac{R}{A} \right)^2} \right) \quad (3)$$

The mathematical exploitation of the aforementioned theory is quite straight forward and permits to predict with a good numerical precision the set of critical parameters and the impact of nonlinear effects amongst others.

## 1.2 Nominal configuration

First the nominal configuration is studied with the original data of [6, 7] for the Space Shuttle's control system. Various ways exist to perform an analysis of such an aircraft pilot system including a nonlinear element such as a rate limiter. Founding works [10], reviews [3] or original illustrations [11] are all of great value in order to accomplish the nonlinear analysis and to understand the pros and cons of each approach.

Here a configuration with direct inputs of the open-loop command channel is chosen as analysis frame. With forced oscillations as stick inputs, the variation of their pulsation permits to show jumps in amplitude but also hysteresis phenomenon since the critical value is not the same with increasing and decreasing pulsations. All these features are illustrated in figure 2.

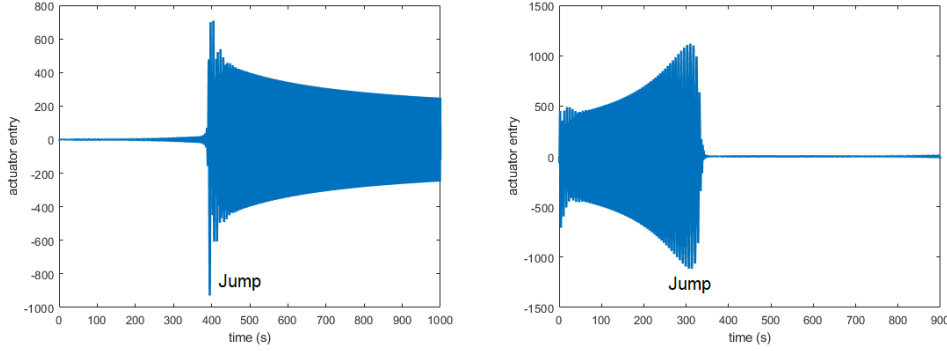


Figure 2 – Time simulations with increasing (left) and decreasing (right) pulsation of stick input forced oscillations. Jump (and hysteresis) phenomena.

Once a global behaviour and catastrophic issues are observed, it is necessary to determine more precisely these different features. In order to better predict the critical values and the evolutions of pulsation  $\omega$ , amplitude  $A$  and dephasing (phase angle  $\phi$ ) of the limit cycles, it is possible to solve an harmonic balance equation like 4 here.

$$Ae^{j\phi} = \frac{Filter(j\omega)}{-1 + N(A, \omega)Actuator(j\omega)(Airframe(j\omega)FeedbackLag(j\omega)Filter(j\omega) + PositiveFeedbackLag(j\omega))} \times Feedforward(j\omega)Input \quad (4)$$

It involves the transfer functions of all the elements of the command channel for the linear part and the describing function  $N(A, \omega)$  of the rate limited element for the nonlinear part and takes into account the relation between them in the Space Shuttle's pitch rate control system. Sometimes the rate limited element is replaced by an equivalent scheme including a saturation. From the mathematical point of view, it is an implicit equation with 3 variables ( $A, \phi$  and  $\omega$ ) and 2 equations (real and imaginary parts of the harmonic balance equation). The numerical computation of the solution is based on a so-called (pseudoarclength) continuation algorithm. Several implementations or conceptions of the algorithm and its associated theory exist [12, 13, 14]. In particular, there are the core of toolboxes devoted to the analysis of dynamical systems which rely on them to compute the curve of equilibria. The other capabilities consist in the detection and specific management of the bifurcations in order to initialize the computation of other branches or to calculate the Lyapounov coefficient (subcritical / supercritical bifurcation) but also in the offered possibility of time integration or in the specific handling of periodical orbits.

The values for which the fold bifurcations of limit cycles occur correspond exactly to the turning points of the curve. Actually there are two stable branches of limit cycles, one of low amplitudes and one of high amplitudes but also one unstable branch of intermediate amplitudes. Moreover the underlying behaviour is put in evidence by means of this graph. Indeed the bifurcations correspond to flying qualities cliffs and imply a sudden jump of oscillation amplitudes after a little variation of pulsation of

the stick input oscillations. Indeed the Space Shuttle cannot follow the unstable branch and must stabilize itself on another stable branch of periodic orbits. The hazardous nature of this situation comes from the surprise effect which can render it difficult to manage for the pilot. Another tricky aspect is the presence of an hysteresis that is to say once jumped on the branch of higher amplitudes, a far lower pulsation is necessary so as to return to the branch of low amplitudes. This fact adds further difficulties since it is completely unintuitive without a priori knowledge and effective decisions must be taken relatively quickly and accurately since it was in an landing phase (near the ground).

### 1.3 DFM and continuation for harmonic balance equation resolution

Since the source of pilot induced oscillations is a rate limited actuator, a nonlinear analysis is required. Indeed linear considerations cannot catch such behaviours. Several methods are available so as to accomplish this and many workshops, projects were devoted to this objective [15, 16] selecting the concrete frontier values employed for each type of flight task (and aircraft). The main remarkable features for control systems with rate limiting are the presence of jumps, so-called *flying qualities cliffs* which can be more or less nasty [8]. Moreover several kinds of bifurcations appear to be responsible for that, mainly saddle-node (fold) bifurcation of limit cycles and Hopf bifurcation of equilibria are observed [17, 18, 10].

In this particular study, the describing function method is employed so as to examine the evolution of periodical orbits. Thus we try to find solutions to the harmonic balance equation thanks to a pseudo-arclength continuation [13, 12]. This last one is an algorithm whose aim is to compute the solutions of a system of implicit (nonlinear) equations. The associated functions must be sufficiently regular and generally there is (only) one variable more than equations. Moreover, other neighbouring problems can also be treated such as the computation of multiple solution branches, the determination of the bifurcation nature, etc.

Concerning the specific problem of forcing oscillatory inputs of the Space Shuttle command channel with a rate limiter, an harmonic balance equation 5 can be solved [19].

$$Ae^{j\phi} = \frac{Filter(j\omega)}{1 - N(A, \omega)Actuator(j\omega)Airframe(j\omega)Feedback(j\omega)Filter(j\omega)}Feedforward(j\omega)Input \quad (5)$$

where  $A$  and  $\phi$  are the amplitude and phase of the entry signal of the rate limiter whose describing function is  $N(A, \omega)$  and  $Input$  the amplitude of the stick inputs. The data are given in [6, 7] and the pure time delay (of value  $T$ ) is approximated by a (classical) 3<sup>rd</sup> order Padé transfer function.

In fact, the equation 6 is really the one to solve (for easy and practical writing of the mathematical relations of the closed-loop system, the "Filter" block can be moved in all the branches in front of the "Sum" block in figure 3).

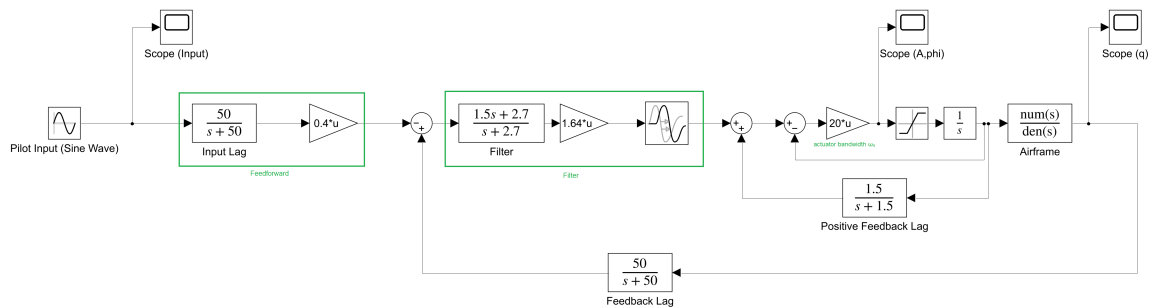


Figure 3 – Control system of the Space Shuttle's pitch attitude with article notations.

$$Ae^{j\phi} = \frac{Filter(j\omega)}{-1 + N(A, \omega) Actuator(j\omega) (Airframe(j\omega) FeedbackLag(j\omega) Filter(j\omega) + PositiveFeedbackLag(j\omega))} \times \frac{Feedforward(j\omega) Input}{(6)}$$

By replacing the rate limiter with the equivalent scheme (figure 1), the harmonic balance equation must be modified with the describing function of the saturation  $N(A)$  and the actuator bandwidth  $\omega_a (= 20 \text{ rad/s}$  here) to obtain equation 7 (where  $A$  and  $\phi$  are the amplitude and phase of the entry signal of the saturation).

$$Ae^{j\phi} = \frac{\omega_a Filter(j\omega)}{-1 + \frac{\omega_a}{j\omega} N(A, \omega) (Airframe(j\omega) FeedbackLag(j\omega) Filter(j\omega) + PositiveFeedbackLag(j\omega))} \times \frac{Feedforward(j\omega) Input}{(7)}$$

The results (for the worst case) with a time delay  $T = 0.4 \text{ s}$  and an input amplitude of  $15^\circ$  are shown in figure 4. The amplitude is expressed in  $dB$  so as to have quite homogeneous values with the other variable units (deg for the phase delay in the bode plots). Indeed the continuation algorithm may encounter some numerical failures if the variables have too different absolute values and an habitual scaling factor may not be sufficient because of the too big range of amplitude values.

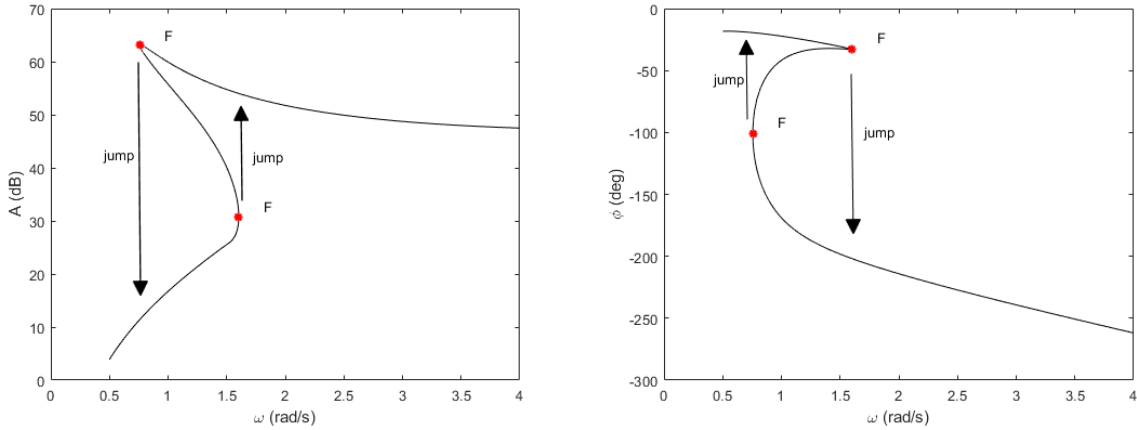


Figure 4 – Amplitude  $A$  and phase  $\phi$  at actuator entry in function of the pulsation  $\omega$  of the pilot inputs according to DFM. Diagnosis of jumps due to a rate limited actuator in the Space Shuttle's command channel.

Some fold bifurcations [20] of periodical orbits are diagnosed and are responsible for sudden jumps. From the flight dynamics viewpoint, these last ones may take the pilot by surprise and lead to an accident. Another issue is that once the branch with higher amplitudes is reached because of a little change of input frequency, a huge decrease in the input frequency is necessary so as to jump back to the branch with lower amplitudes. This hysteresis phenomenon may render the situation quite difficult to tackle in-flight.

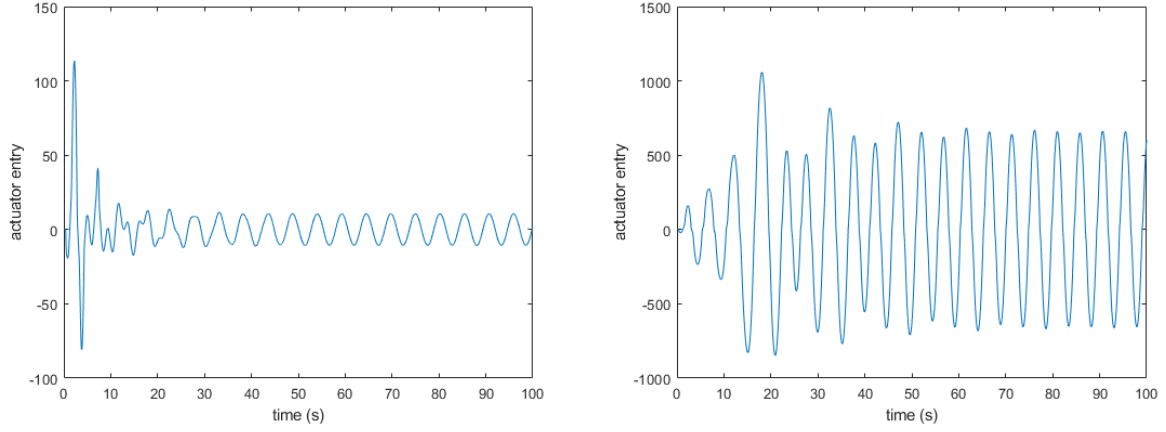


Figure 5 – Time simulations at actuator entry for pilot inputs of amplitude  $15^\circ$  and of pulsation  $\omega = 1.2 \text{ rad/s}$  (left) and  $\omega = 1.3 \text{ rad/s}$  (right). Stabilization to the branch of low amplitude or to the one of high amplitude.

In figure 5, the time simulations realized for different input pulsations ( $\omega = 1.2 \text{ rad/s}$  and  $\omega = 1.3 \text{ rad/s}$ ) are converging towards the limit cycle of low amplitude or high amplitude. If this jump occurs, the pilot may be astonished. But the time simulations show that once a second limit cycle exists, the switch to the high amplitudes can happen anytime. This may create a dangerous situation and a linear analysis is far from predicting such an unpleasant occurrence.

## 2. Feedback loop for PIO alleviation

When trying to cope with PIO problems due to rate limiting, the most direct way consists in adapting the sensitivity of the stick and thus to adapt the shaping function. A first proposal is made at the end of the technical memorandum [6] and another one is exposed in the other technical report of the same author. Moreover, it is also possible to add a feedback block so as to re-use the PID tuning know how. Some classical techniques will next be employed so as to design several types of feedback loops. Their effectiveness may be evaluated thanks to time simulations with specific inputs. But continuation methods will be preferred in this study. Amongst others, the corrections of the nominal configurations are based on PID and back-calculation. Many works were devoted to conceive Phase Compensated Rate Limiters (PCRL) [21], etc. There are mainly linear but can possibly contain nonlinear elements in it such as nonlinear gains, dead zone, saturations, rate limiter, etc. Sometimes it is the feel system which is conceived with a nonlinear sensitivity to manage the issue. This possibility will also be evoked and examined.

### 2.1 PID feedback

For example, when adding a PID block before the lead-lag filter, we may hope to change sufficiently the dynamics by a fine tuning so as to modify the reaction to strong solicitations in the stick. In the next configuration a PID under the form  $PID(s) = k_p + \frac{k_i}{s} + k_d \frac{s}{T_f s + 1}$  is selected. A comparison is made between the nominal configuration and the one with this modification for forced oscillations of amplitude  $5 \text{ deg}$  as input (and a time delay of  $0.5 \text{ s}$ ) and is illustrated in the figures 6.

### 2.2 Feedback of the input/output difference (back-calculation)

A direct anti-windup strategy consists in measuring the difference of the input and the output of the rate-limited element, than to filter the signal with a low-pass filter and to apply the little correction at the entry like described in the modified command channel (figure 7). The effects can be direct and are illustrated in the time simulations figure 8.



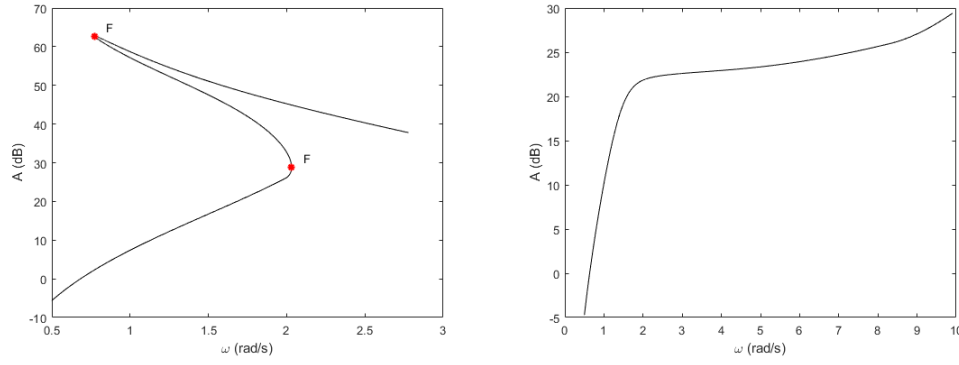


Figure 6 – Influence of a PID in a command channel without (left) or with it (right). Presence or absence of jumps for the Space Shuttle’s command channel with forced inputs as shown by the diagrams presenting amplitude  $A$  (of the periodical orbit) in function of pulsation  $\omega$ .

The harmonic balance equation 5 can be adapted to incorporate a feedback loop which takes into account the difference between input and output of saturated element.

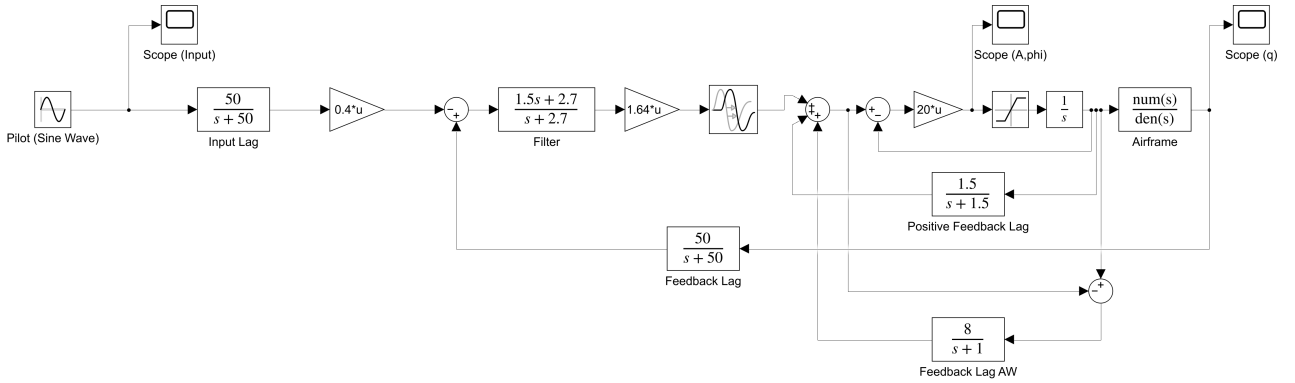


Figure 7 – Low-pass filter correction applied to a command channel and taking into account the difference between the input and the output of the rate-limited actuator.

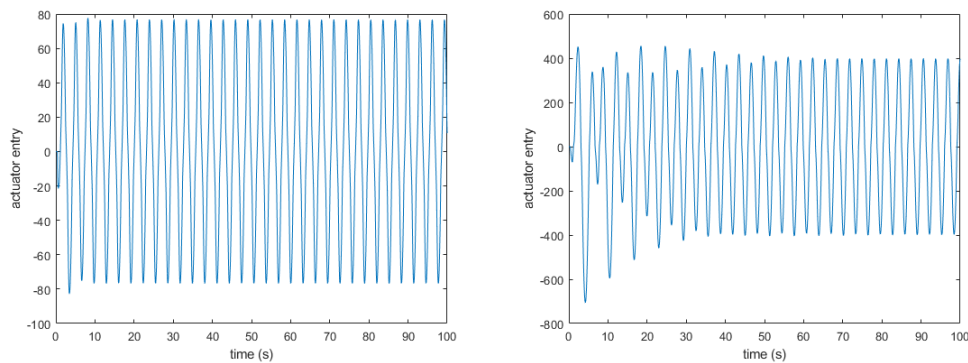


Figure 8 – Influence of a low-pass filter correction. Time simulations for an input of amplitude  $15^\circ$  and pulsation  $\omega = 2 \text{ rad/s}$ . Disappearance of jumps with the feedback correction (left) in comparison with the original command channel (right).

By adapting equation 5 so as to employ the describing function method and a continuation algorithm, it is possible to determine the (first harmonic) characteristics of the periodical orbits at the entry of the actuator saturation in function of the input pulsation for this specific case with a sole feedback loop.

With the low-pass filter  $Filter_{AW}(s) = \frac{8}{s+1}$  in the feedback loop (back-calculation) of the attitude control system as shown in figure 7, harmonic balance equation becomes

$$Ae^{j\phi} = -\frac{Feedforward(j\omega)Before(j\omega)}{1+Filter_{AW}(j\omega)}\omega_a Input + \omega_a \left( \frac{1}{j\omega} \frac{-1+Filter_{AW}(j\omega)+PositiveFeedbackLag(j\omega)}{1+Filter_{AW}(j\omega)} + \frac{Airframe(j\omega)Feedback(j\omega)Before(j\omega)}{1+Filter_{AW}(j\omega)} \right) Ae^{j\phi} N(A, \omega)$$

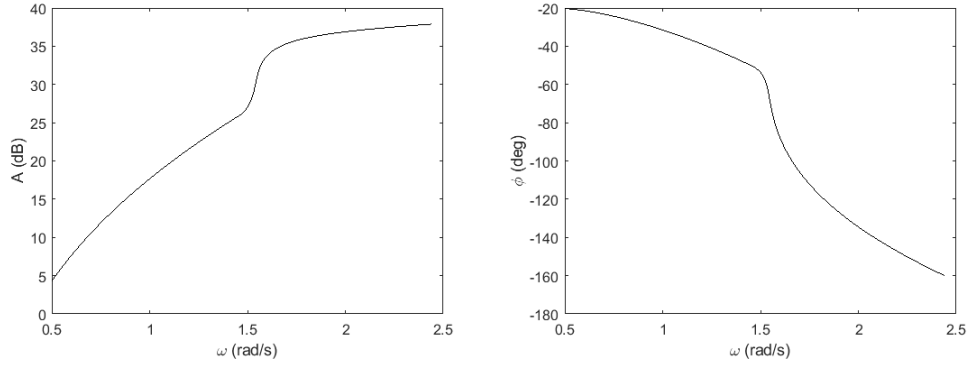


Figure 9 – Diagrams presenting amplitude  $A$  and phase  $\phi$  (towards forced oscillations inputs) of the periodical orbit at actuator entry in function of pulsation  $\omega$  for the pitch attitude control system with a low-pass filter correction according to DFM.

This last simple anti-windup technique has bad reputation for the high frequencies and is thus often extended with a bypass [22]. But here it seems to offer sufficient effects to tackle this issue.

In the bifurcation diagram (figure 9), the bifurcation points have disappeared (in comparison with the nominal configuration). This indicates that this feedback loop is sufficient enough to cope with the flying qualities cliffs. There remains just a huge increase in amplitude (or decrease in phase) which may still cause some disturbances for the pilot, but it must be manageable.

The interest of these nonlinear analysis tools are clearly shown, since they permit to know in advance whether a configuration might be hazardous or not as regards PIO or PIO-like phenomena. Once the methodology and the numerical tools are adapted and implemented, it is possible to compute systematically the different control systems, the limitations (numerical values or types of command channels) being known in advance by experience.

After analysing the nominal configuration and putting in evidence all the characteristic features of this configuration, the impact of some design parameters will be assessed next.

### 2.3 Design parameter

One design parameter is the overall time delay. Intuitively the higher this last one is, the more likely nefast phenomena may happen. Contributions can come from almost every element since mechanical pieces, analog-digital converter, computations, etc are all adding some delay. The practical engineering question is to determine when it becomes too big and no more manageable. A mathematical analysis is performed here which can help preparing future flight tests or simulator sessions by indicating in advance the configurations which are problematic. Amongst others we try to assess how the limit cycles are evolving with regards to this parameter by considering first the bifurcation diagram (locus of equilibria) which allows to catch the behavioural specificities and then the locus of the bifurcation points which permits to delimit the dangerous zone.

The overall delay has a huge impact on the global behaviour of the command channel. Combined with the main effects of rate limiting, it favours the apparition of jumps, destabilizations. Therefore a



question remains to assess when the degradation of the flying qualities is so nefast that the space shuttle becomes uncontrollable (or very difficultly). The typical diagrams of bifurcation theory resume well the different situations and furnishes the critical values associated to the behavioural changes.

The periodical orbits for a delay of  $T = 0.4s$  were already analysed in the previous sections. The other configurations need also to be examined, especially with other delays, between  $0s$  and  $0.4s$  for example.

The locus of bifurcation points (figure 10) delimits the zone of control parameters (input pulsation, delay) for which multiple periodical orbits exist. Outside of this hatched region, there is just one single stable periodical orbit (classical situation) whereas in this hatched zone, there are two stable limit cycles and an unstable limit cycle. From the behavioural point of view, jumps may happen, implying flying qualities cliffs. This represents the major risk which is diagnosed and requires some further attention. We can see from which values such behavioural drops happen, particularly the critical overall time delay  $T$  of the command channel.

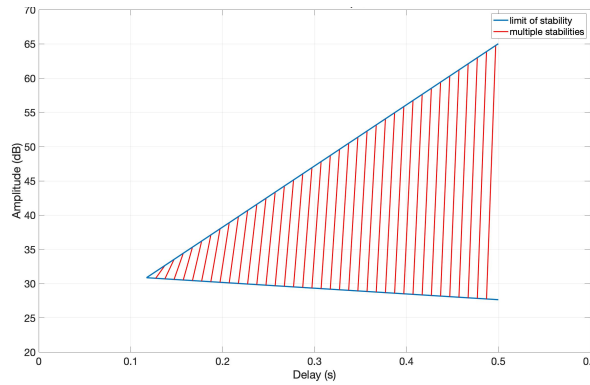


Figure 10 – Locus of bifurcation points for a sinusoidal input of  $5^\circ$  amplitude. Cusp projected in the plane (Delay  $T$ , Amplitude).

The associated surface of equilibria would look like a cusp in the space (Delay  $T$ , Pulsation, Amplitude) whose projection in the plane (Amplitude, Delay  $T$ ) is shown in figure 10. More generally we can note that the higher the time delay is, the more likely nefast situations can happen (which confirms a quite intuitive result). The precise delimitation of these nasty aircraft reactions is helpful because it permits both to warn the pilot of forecoming problems and to make the engineer observe the impact of modifications (of the command channel) on the overall flight dynamics.

The first topic dealt with the pilot induced oscillations of the Space Shuttle and its mathematical analysis. The second one will look at identifying flight phases of transport airplanes.

### 3. Identification of the flight phases of transport airplanes

Another topic of this study deals with the identification of a flight model or of flight phases. Apart from the mathematical structure of the model and the exploitation of an optimization algorithm [23], the level of instrumentation and the measure availability of physical variables have an impact over the methodology to choose. In order to exploit artificial intelligence, an initial work exploits data coming from air traffic management (since there are freely available, the creation of a training database is easy).

There are several steps in order to successfully identify an aircraft model. First the structure of the model must be adequately chosen, then the types of inputs and their sequence must be relevant. Finally the mathematical identification algorithm must be adequately parametrized. At the end, they must furnish significant results.

Here we present some results relative to the lateral flight dynamics. Actually we try to evaluate the aerodynamic derivatives of the lateral flight dynamics. The classical inputs such as described in [23, 24] are applied to aircraft models furnished by [25, 26, 27]. The inputs are pulse, (doublet,) and the so-called 3 – 2 – 1 – 1 like indicated on the figure 11. Exploiting the data obtained thanks to simulated flights, the different trials and their results are exposed in what follows.

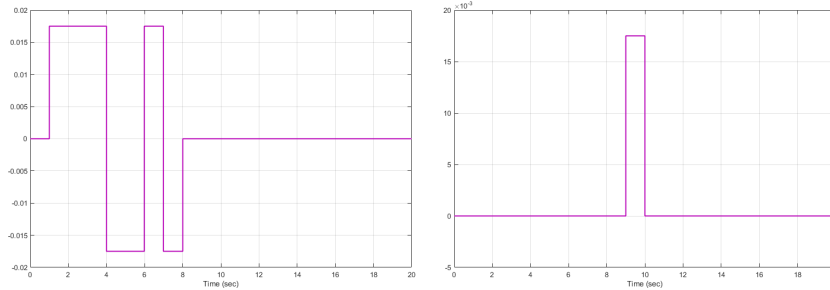


Figure 11 – Inputs on aileron (left) and rudder (right) for the (simulated) flight tests.

For simplification reason, it would be desirable to obtain all the data with one single optimization. But it must be admitted that these attempts were unsuccessful. Even by taking care of exciting all the possible modes by inputs on ailerons and rudder and by making diverse attempts with diverse options of the identification toolbox, the results were not satisfactory. That's why it is preferable to decompose the motion on the axes of roll and yaw having an idea in advance of the associated time constant.

There remains the question of the representation employed that is to say a transfer function or a state space model and of the algorithm. For the identification of several transfer functions at the same moment, with the *tfest* function of the *identification toolbox* [28] of *matlab*, the main problem is that the denominators of the transfer function are not the same for the different variables (over an identical control). It is thus unexploitable, the eigenmodes characterization being one of the key aspects of the identification process.

That's why it seems more reasonable to identify a state space model with the *ssest* function of the *identification toolbox* [28] of *matlab*. The Levenberg-Marquardt (LM) algorithm is selected with the canonical form as option, which is a common choice but which seems to work quite effectively (compared to attempts with other available search methods and options). Nevertheless full matrices of state, control and observation have too many coefficients implying the identification/optimization algorithm to fail. A rare success is furnished on the figure 12. Some constraints are added to nullify some matrix coefficients or to force them to zero (or one).

Moreover a separation can be made between the roll and yaw axes on the one side and between the short and slow motions on the other side. This decoupling already looks like a better approach, even if it nullifies all the coupling matrices and fixes some negligible aerodynamic derivatives to zero right from the beginning.

For the practical application, several flight cases were used. One is taken from a Douglas DC-8 aircraft (total weight of 190 000 *lb* and flying at Mach 0.44 at an altitude of 15000 *ft*) in the textbook [25]. But another one could come from a Boeing 747 whose data are available amongst others in the NASA report [27].

At the end, it is possible to reconstruct the lateral flight model with a reasonable error and with an estimation of it. In this case, since we have a priori information of the model, it is possible to compare the initial values to the results. But the criteria to assess whether an identification is successful or not would also merit to be debated. Nevertheless we see that the options taken so as to make the identification of the lateral dynamics seems to give adequate results with regards to the time

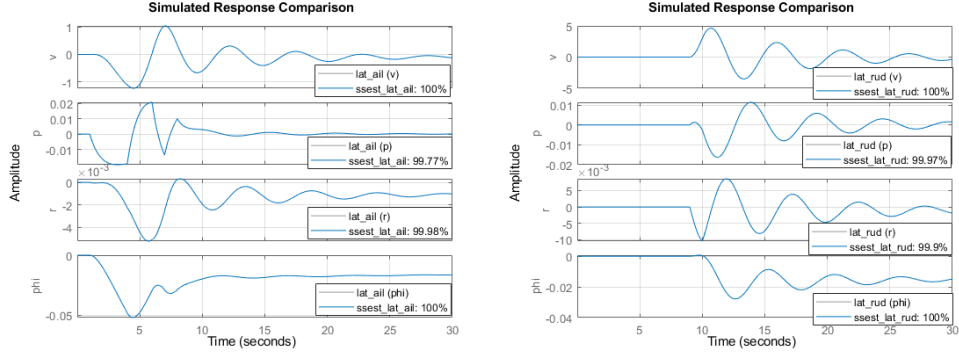


Figure 12 – Identification after inputs on the roll control (left) and on the yaw control (right) with (coupled) 4-state model.

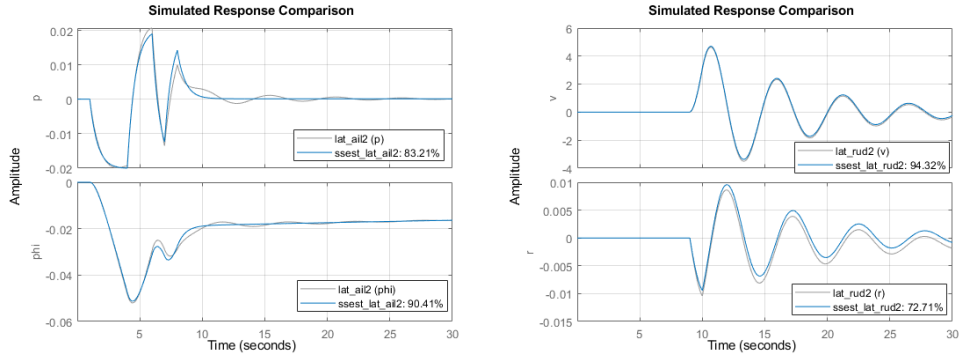


Figure 13 – Identification after inputs on the roll control (left) and on the yaw control (right) with decoupled 2-state models.

simulations associated to the initial and identified models in figure 13. Normally by applying such inputs and by limiting the number of aerodynamic derivatives to determine, it seems possible to converge to the correct values. The chosen state variables are  $X = (v, r, p, \phi)$  (lateral component of airspeed, yaw rate, roll rate, bank angle) and the controls are  $U = (\delta_a, \delta_n)$  (aileron, rudder). The decoupling on the roll and yaw axes traduces itself by reducing the problem to the evaluation of space representations with only 2-state vectors i.e.  $X_{roll} = (p, \phi)$  and  $X_{yaw} = (v, r)$ . Moreover we can also worry about the robustness of the process towards noise. Indeed it is unavoidable to get noisy measurements, that's why verifying if everything is not collapsing in this case is also important.

With reasonable noise, it seems possible to apply the procedure of identification. The noise follows a centered normal distribution. The level of error is obviously higher, but the obtained values remain correct. In the figures 14 (inputs on the roll control) and 15 (inputs on the yaw control), the trajectories with the identified and the initial models are compared (with or without noise).

Concerning a completely different subject which the identification of flight phases, an initial work is done which can be helpful nevertheless. Indeed once it works, it can reduce significantly the time lost by pilots and technicians in annotating and classifying segments of flights.

One of the major problems when exploiting artificial intelligence is often the creation of a reliable training database. This obstacle is circumvented by choosing an application with freely available data that is to say coming from air traffic control and the ADS-B messages sent by a mandatory transponder. Moreover the training and prediction of a neural network permit to determine the type of phase in which a transport airplane is evolving. For this last part, data corresponding to air traffic are taken from flight tracker web site for example. After being pre-treated so as to be exploitable and eventually

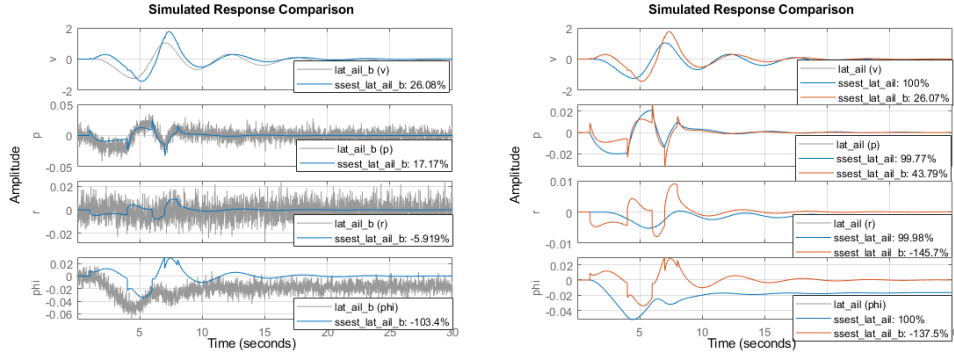


Figure 14 – Identification after inputs on the roll control with or without noise.

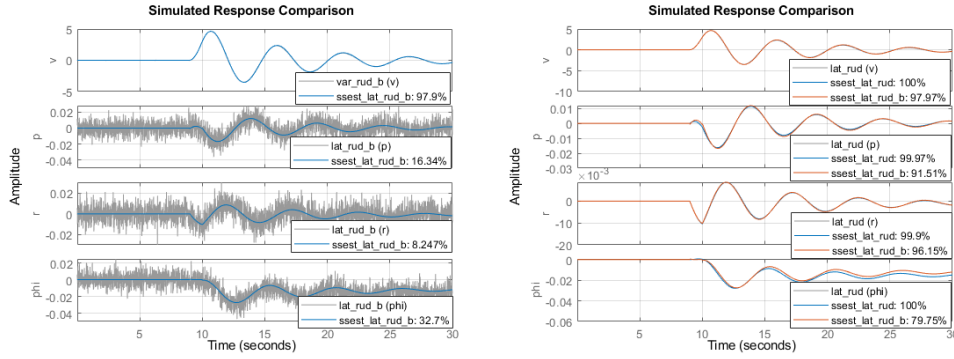


Figure 15 – Identification after inputs on the yaw control with or without noise.

annotated (and even other variables may be calculated), hyperparameters characterizing the neural network must be chosen adequately to construct a neural network (supervised or not). Once it works, it can reduce significantly the time lost by pilots and technicians in annotating and classifying segments of flights.

The *Scikit-Learn* (*SkLearn*) package of *Python* is employed for the neural network processing. A first test uses the flight database freely at disposal [kilthub.cmu.edu/articles/dataset/TrajAir\\_A\\_General\\_Aviation\\_Trajectory\\_Dataset/14866251](http://kilthub.cmu.edu/articles/dataset/TrajAir_A_General_Aviation_Trajectory_Dataset/14866251). We must choose the number of hidden layers and of neurons, the learning rate. 80% of the available data are exploited in order to train the neural network and the remaining 20% to evaluate its effectiveness in the prediction. Concerning the fields present in the original database, the flight path or the climb rate was added (by calculation) to the (ground) speed and the altitude. It is also possible to treat sole flight point or to segment the flight with a regular duration (mean values over a flight segment). The neural network can also be chosen as supervised or not supervised. In the first case, the items of the database are annotated with labels indicating the type of cruise, whereas in the second case, the neural network generates itself the different categories without a priori knowledge of the characteristics of the different flight phases. For the supervised case, strategies must be developed to give a correctly label to the different items. For example, we must choose to consider isolated data at certain flight moment or segments of several seconds of flight but also if other information should be added to the initial data furnished. Often there are only trajectory information such as (ground) speed and altitude. In order to make the discrimination of the flight phases, it may be helpful to include the values of the flight-path angle or climb rate. At the end, the success rates are furnished in the confusion matrices. For this simple application, only 3 phases are distinguished that are level flight, climb and descent. The diverse classifiers at disposal in the *Scikit-Learn* package are exploited like Support Vector Machine (SVM), Artificial Neural Networks (ANN), Gaussian Naive Bayes (GNB), Decision Tree, Random Forest, etc.

Table 1 – Confusion matrix for GNB

		True diagnosis		
		Level flight	Climb	Descent
Test	Level flight	0.25	0	0
	Climb	0	0.25	0
	Descent	0	0.25	0.25

Table 2 – Confusion matrix for SVM

		True diagnosis		
		Level flight	Climb	Descent
Test	Level flight	0.25	0	0
	Climb	0	0.5	0
	Descent	0	0	0.25

In the confusion matrices (tables 1 and 2) obtained when testing small samples of aircraft traffic data with GNB or SVM, the results seem quite reasonable, since there are a limited number of false evaluations. Thus after this premier attempt of AI exploitation for flight dynamics identification, we can state that such a tool seems helpful and effective for the automatic classification of flight phases. We could also exploit unsupervised machine learning with the mean shift method for example.

## Conclusion

Several topics were tackled in this study and involved flight dynamics and applied mathematics. First of all, the pilot induced oscillations of the Space Shuttle are examined by means of tools devoted to the analysis of nonlinear phenomenon. Bifurcation theory, harmonic balance, describing function, continuation algorithm are all exploited so as to diagnose the critical values and to extract the important features of the underlying dynamics. A parametric study (on the overall time delay) is also accomplished aiming at circumscribing the dangerous region of parameters. Having an idea of the critical value of a parameter before a global behaviour change appears is also an important clue for the design and the comprehension of an aircraft command channel. Furthermore the nonlinear analysis of modified control systems puts in evidence the eventual disappearance or attenuation of undesirable effects. Secondly the lateral flight dynamics model of transport airplanes were identified and methodological choices were highlighted. The options needed for the identification algorithm and the decomposition of the initial issue in several subsystems by making decoupling assumptions is a reasonable way to come to a successful identification of the global model. Thirdly neural networks were employed in order to discriminate the different flight phases of airliners. For this application, some tuning of the hyperparameters of neural network are made and information, supplementary variables are added at the initial database provided by air traffic control. All in all mathematical tools and practical flight dynamics considerations permit to obtain valuable information for the design and exploitation of aircraft.

## Acknowledgements

I warmly thank all my trainees in master degree for their contributions to the different topics presented here.

## Contact Author Email Address

email: [sebastien.kolb@ecole-air.fr](mailto:sebastien.kolb@ecole-air.fr)

## Copyright Statement

The authors confirm that they, and/or their company or organization, hold copyright on all of the original material included in this paper. The authors also confirm that they have obtained permission, from the copyright holder of any third party material included in this paper, to publish it as part of their paper. The authors confirm that



they give permission, or have obtained permission from the copyright holder of this paper, for the publication and distribution of this paper as part of the ICAS proceedings or as individual off-prints from the proceedings.

## References

- [1] David Howard Klyde. *Pilot-Induced Oscillations and Control Surface Rate Limiting: Comprehension, Analysis, Mitigation, and Detection*. PhD thesis, Delft University of Technology, 2022.
- [2] David H. Klyde and David G. Mitchell. Investigating the role of rate limiting in pilot-induced oscillations. *Journal of Guidance, Control, and Dynamics*, 27(5):804–813, 2004.
- [3] Various. Flight control design - best practices. Technical Report 10.14339/RTO-TR-029, RTO, 2000.
- [4] E. Field, W. von Klein, R. van der Weerd, and S. Bennani. The prediction and suppression of pio susceptibility of a large transport aircraft. In *Atmospheric Flight Mechanics Conference*, Denver, Colorado, August 2000. AIAA.
- [5] Marilena D. Pavel, Michael Jump, Binh Dang-Vu, Pierangelo Masarati, Massimo Gennaretti, Achim Ionita, Larisa Zaichik, Hafid Smaili, Giuseppe Quaranta, Deniz Yilmaz, Michael Jones, Jacopo Serafini, and Jacek Malecki. Adverse rotorcraft pilot couplings - past, present and future challenges. *Progress in Aerospace Sciences*, 62:1–51, 2013.
- [6] J.W. Smith. Analysis of a longitudinal pilot-induced oscillation experienced on the approach and landing test of the space shuttle. Technical Memorandum TM-81366, NASA, 1981.
- [7] Duc H. Nguyen, Mark H. Lowenberg, and Simon A. Neild. Effect of actuator saturation on pilot-induced oscillation: A nonlinear bifurcation analysis. *Journal of Guidance, Control, and Dynamics*, 44(5):1018–1026, 2021.
- [8] Holger Duda. Prediction of pilot-in-the-loop oscillations due to rate saturation. *Journal of Guidance, Control, and Dynamics*, 20(3):581–587, 1997.
- [9] A. Gelb and W. E. Vander Velde. *Multiple-Input Describing Functions and Nonlinear System Design*. McGraw Hill, New York, 1996.
- [10] R. Mehra and R. Prasanth. Bifurcation and limit cycle analysis of nonlinear pilot induced oscillations. In *23rd Atmospheric Flight Mechanics Conference*, Boston, Massachusetts, August 1998. AIAA.
- [11] Maide Bucolo, Arturo Buscarino, Luigi Fortuna, and Salvina Gagliano. Bifurcation scenarios for pilot induced oscillations. *Aerospace Science and Technology*, 106:106194, 11 2020.
- [12] A. Dhooge, W. Govaerts, and Yu. A. Kuznetsov. Matcont: A matlab package for numerical bifurcation analysis of odes. *ACM Trans. Math. Softw.*, 29(2):141–164, jun 2003.
- [13] Eirik Ravnas. Continuation and bifurcation software in matlab. Master's thesis, NTNU, 2008.
- [14] Bard Ermentrout. Simulating, analyzing, and animating dynamical systems: A guide to xppaut for researchers and students. *Applied Mechanics Reviews*, 56, 07 2003.
- [15] AGARD. *Flight Control Design - Best Practices*. Number RTO-TR-029. North Atlantic Treaty Organization, 2000.
- [16] FM(AG12). Analysis of nonlinear pilot-vehicle systems using modern control theory. Technical Report TP-120-02, GARTEUR, 2000.
- [17] Francisco Gordillo, Ismael Alcalá, and Javier Aracil. Bifurcations in systems with a rate limiter. In Fritz Colonius and Lars Grüne, editors, *Dynamics, Bifurcations, and Control*, pages 37–50, Berlin, Heidelberg, 2002. Springer Berlin Heidelberg.
- [18] I. Alcalá, F. Gordillo, and J. Aracil. Saddle-node bifurcation of limit cycles in a feedback system with rate limiter. In *2001 European Control Conference (ECC)*, pages 354–359, 2001.
- [19] S. Kolb. Flight dynamics analysis and trajectory optimization of some gliding phases. In *Aerospace Europe Conference 2023 - 10<sup>th</sup> EUCASS - 9<sup>th</sup> CEAS*, july 2023.
- [20] John Guckenheimer and Philip Holmes. *Nonlinear oscillations, dynamical systems, and bifurcations of vector fields*, volume 42 of *Applied Mathematical Sciences*. Springer-Verlag, New York, 1983.
- [21] Eric R. Kendall. Phase compensated rate limiters for alleviation of pilot-induced oscillations caused by control surface rate limiting. *SAE Transactions*, 114:1427–1431, 2005.
- [22] L. Rundqwist. Rate limiters with phase compensation. In *Proceedings of 20th Congress of ICAS*, 1996.
- [23] Ravindra Jategaonkar. *Flight Vehicle System Identification: A Time Domain Methodology*, volume 216 of *Progress in Astronautics and Aeronautics*. AIAA, 08 2006.
- [24] Eries Bagita Jayanti, Fuad Surastyo Pranoto<sup>1</sup>, and Singgih Satrio Wibowo. Identification of aircraft parameters in the lateral-directional flight dimension with variation of control input. *Jurnal Teknologi Dirgantara*, 20(1), 2022.



- [25] M. V Cook. *Flight dynamics principles : a linear systems approach to aircraft stability and control*. Elsevier aerospace engineering series. Butterworth-Heinemann, Waltham, MA, 3rd ed edition, 2013.
- [26] B.L. Stevens and F.L. Lewis. *Aircraft Control and Simulation*. Wiley, 2003.
- [27] Robert Heffley and W. Jewell. Aircraft handling qualities. Technical Report NASA-CR-2144, NASA, 1973.
- [28] Lennart Ljung. System identification toolbox<sup>TM</sup> user's guide. Technical report, Mathworks, 2023.